


# Prediction of late displacement of the globe in orbital blowout fractures

Yongrong Ji,<sup>1,2</sup> Yixiong Zhou,<sup>1,2</sup> Qin Shen,<sup>1,2</sup> Wei Xu,<sup>1,2</sup> Shengfang Ge,<sup>1,2</sup> Lixu Gu<sup>3</sup> and Xianqun Fan<sup>1,2</sup> 

<sup>1</sup>Department of Ophthalmology, Ninth People's Hospital, Shanghai Jiao Tong University School of Medicine, Shanghai, China

<sup>2</sup>Shanghai Key Laboratory of Orbital Diseases and Ocular Oncology, Shanghai, China

<sup>3</sup>School of Biomedical Engineering, Shanghai Jiao Tong University, Shanghai, China

## ABSTRACT.

**Purpose:** To establish a linear measuring method in computed tomographic (CT) images to predict the displacement of the globe late after orbital blowout fracture.

**Methods:** Subjects were retrospectively included. Inclusion criteria were as follows: (1) adult subjects ( $\geq 18$  years old at the time of trauma); (2) unilateral orbital medial-wall and/or floor fractures; (3) CT examination at least 30 days after trauma. Exclusion criteria were as follows: (1) facial or orbital fracture extending to other parts of the orbit than medial-wall and/or floor; (2) history of orbital or ocular abnormality other than the orbital trauma; (3) severe ocular trauma accompanied by the orbital trauma; (4) orbital fracture treated surgically before the CT examination. A co-ordinate system was built based on the orbital CT scans. Displacements of orbital walls, displacement of the globe and relative location of the fracture site were measured. Correlations between the variables were investigated.

**Results:** Ninety-nine per cent of fracture sites of the medial wall and 100% of fracture sites of the floor were posterior to the centre of the unaffected globe. The affected globe moved significantly medially ( $p < 0.001$ ) and backwards ( $p < 0.001$ ) in pure medial-wall fracture; backwards ( $p < 0.001$ ) and downwards ( $p = 0.017$ ) in pure floor fracture; and medially ( $p < 0.001$ ), backwards ( $p < 0.001$ ) and downwards ( $p < 0.001$ ) in medial-wall and floor fractures. Displacement of the globe was correlated with displacements of the orbital walls, and the regression formulae were therefore fitted. Application of the formulae revealed that the same extent of orbital wall displacement caused more displacement of the globe in female patients than in male patients.

**Conclusions:** A linear measuring method in a three-dimensional co-ordinate system was established to identify the displacements of orbital walls and the displacement of the globe in orbital blowout fractures. The regression formulae generated in this study might be used in clinical practice to predict late displacement of the globe by measuring the displacements of orbital walls.

**Key words:** displacement of the globe – linear measurement – orbital blowout fracture – three-dimensional co-ordinate system

Acta Ophthalmol. 2020; 98: e197–e202

© 2019 Acta Ophthalmologica Scandinavica Foundation. Published by John Wiley & Sons Ltd

doi: 10.1111/aos.14226

## Introduction

Orbital blowout fracture is one of the most frequent facial fractures, since the orbital walls, especially the medial wall and the floor, are vulnerable to external force (Catone et al. 1988; Waterhouse et al. 1999). The fracture may result in entrapment of extraocular muscles and herniation of orbital contents, which are the two main indications for surgery (Courtney et al. 2000; Brady et al. 2001; Boyette et al. 2015). Entrapment of extraocular muscles generally leads to ocular motility dysfunction and diplopia. Herniation of orbital contents into the maxillary/ethmoid sinuses may cause displacement of the globe, referred to as enophthalmos. However, estimating the exact displacement of the globe caused by fracture is difficult because post-traumatic intraorbital oedema frequently develops and persists for at least 7–10 days, interfering with the position of the globe early after fracture (Yab et al. 1997; Courtney et al. 2000; Lee & Lee 2016). Thus, many attempts have been made to predict late displacement of the globe by measuring the extent of fracture. The area of fracture defect, increase in total orbital volume and volume of herniated orbital contents have been found to correlate with late onset of enophthalmos (Whitehouse et al. 1994; Yab et al. 1997; Ramieri et al. 2000; Cunningham et al. 2005; Zhang et al. 2012; Sung et al. 2013; Choi et al. 2016a,b; Lee & Lee 2016; Cha et al. 2017; Sugiura et al. 2017). However, these

predictive models are mostly used in research because the measurement of area or volume may be too time-consuming or unfeasible in clinical practice if specific software is not available. Moreover, the extent of enophthalmos, which indicates backward displacement of the globe, has generally been the only variable considered; horizontal and vertical displacements have seldom been considered, even though they also may be present.

Therefore, the aim of this study was to establish a linear measuring method in computed tomographic (CT) images to predict displacement of the globe late after orbital blowout fracture. This predictive model is intended to be suitable for clinical application.

## Patients, Materials and Methods

### Study subjects

Subjects were patients who had been referred to Shanghai Ninth People's Hospital from 1 January 2014 to 31 December 2018 for consultation regarding orbital blowout fracture and who underwent orbital CT scans with slice thickness of 1 mm in this hospital. The patients' medical records and CT scan reports were reviewed. We collected background information of the patients (age, gender), the time and detailed account of the trauma, and the method of treatment. Patients who met the inclusion criteria but not the exclusion criteria were consecutively included in the study.

Inclusion criteria were as follows:

- 1 adult subjects ( $\geq 18$  years old at the time of trauma)
- 2 unilateral orbital medial-wall and/or floor fractures
- 3 CT examination at least 30 days after trauma

Exclusion criteria were as follows:

- 1 facial or orbital fracture extending to other parts of the orbit than the medial wall and/or floor
- 2 history of orbital or ocular abnormality other than the orbital trauma
- 3 severe ocular trauma accompanying the orbital trauma
- 4 orbital fracture treated surgically before the CT examination

The research permit was number SH9H-2018-T41-2. The Medical Ethics Committee of Shanghai Ninth People's Hospital did not require informed consent for this retrospective study. The research adhered to the tenets of the Declaration of Helsinki.

### CT data acquisition

The images of orbital CT scans were collected from the hospital's CT database. Scans were obtained on a 64-row multi-slice CT device (Philips Brilliance), using high-resolution contiguous sections in an axial plane with these criteria: slice thickness, 1.00 mm; field of view,  $25 \times 25$  cm; and matrix,  $512 \times 512$ . All scan images were saved in DICOM format for analysis.

### Measurements of variables in orbital co-ordinate system

Images were analysed with SIMMED software (Shanghai Jiao Tong University, China). To make the measurements in a standard and precise way, a three-dimensional (3D) orbital co-ordinate system was built for the CT images, according to the protocol created in our previous study (Ji et al. 2018). Horizontal planes were set parallel to the Frankfort plane, which is the reference scanning plane of standard orbital CT examination (Lundström & Lundström 1995). The midsagittal reference plane was set perpendicular to horizontal planes and passed through facial midline landmarks (nasion and prechiasmatic groove). The prechiasmatic groove was set as the origin of the co-ordinate system. The coronal planes and the co-ordinate axes were then automatically reformatted since the origin, horizontal planes and sagittal planes were fixed. Computed tomographic (CT) images were adjusted to this co-ordinate system. Each point in the co-ordinate system had an *x*-axis, *y*-axis and *z*-axis co-ordinate.

The mirror co-ordinates of the unaffected globe were set as the control to determine the original position of the globe on the affected side. The displacement of the affected globe was the co-ordinate difference between the current position of the globe centre and its original position (Fig. 1). The mirror boundary of the unaffected orbit was considered as the original boundary of the orbit on the affected side. The

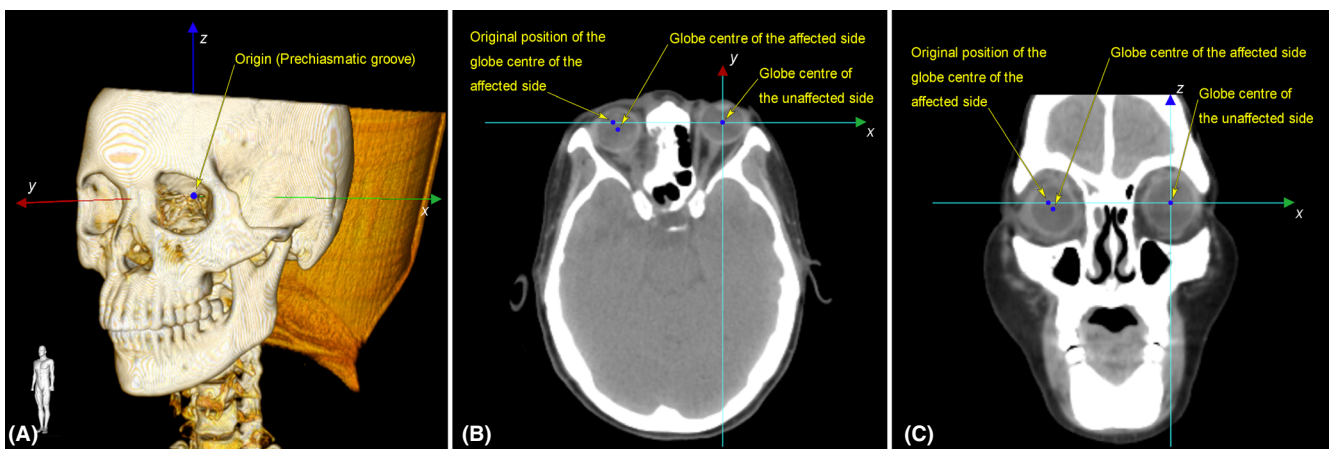


**Fig. 1.** Displacement of the affected globe in three-dimensional (3D) orbital co-ordinate system. (A) Establishment of 3D orbital co-ordinate system on reconstructed skull: origin (prechiasmatic groove), *x*-axis, *y*-axis and *z*-axis. (B, C) Locations of the landmarks on horizontal plane (B) and coronal plane (C). The original position of the globe centre of the affected side is defined as the mirror point of the globe centre of the unaffected side. The displacement of the affected globe is the co-ordinate value difference from the current position of the globe centre to its original position; these two points may not be on the same horizontal plane or coronal plane.

horizontal farthest fracture segment or soft tissue herniated into the ethmoid sinus from the original boundary of the orbit was defined as the fracture site of the medial wall; the vertical farthest fracture segment or soft tissue herniated into the maxillary sinuses from the original boundary of the orbit was

defined as the fracture site of the floor. The displacement of the affected medial wall was the horizontal distance from the fracture site to the original position of the affected medial wall; the displacement of the affected floor was the vertical distance from the fracture site to the original position of the affected

floor. The measurements were taken in coronal planes and checked in horizontal/sagittal planes (Fig. 2). A comparison of the anteroposterior coordinates of the fracture site and the contralateral globe centre determined the relative location (anteroposterior) of the fracture site (Fig. 2B,D).

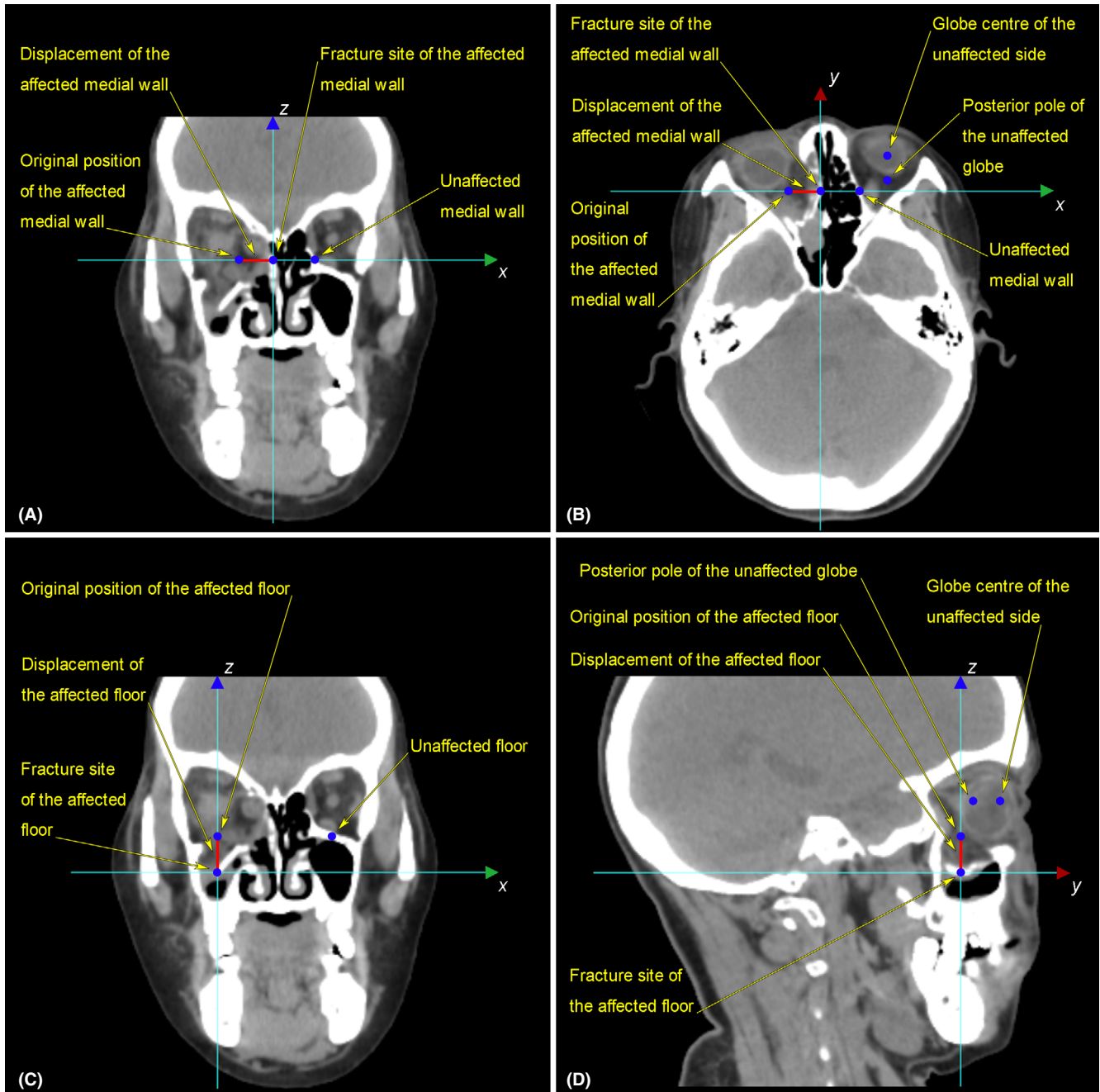


**Fig. 2.** Locations of the fracture sites and displacements of the affected orbital walls. (A, B) Landmarks of medial-wall fracture on coronal plane (A) and horizontal plane (B). The original position of the affected medial wall is defined as the mirror point of the unaffected medial wall on the same *x*-axis (horizontal axis) with the fracture site. The displacement of the affected medial wall is the horizontal distance from the fracture site to the original position of the affected medial wall. The location of the fracture site of the affected medial wall is posterior to the posterior pole of the unaffected globe in this case (B). (C, D) Landmarks of floor fracture on coronal plane (C) and sagittal plane (D). The position of the unaffected floor is defined as the point on the contralateral floor which has the opposite *x*-coordinate to the fracture site. The original position of the affected floor is the mirror point of the unaffected floor. The displacement of the floor is the vertical distance from the fracture site to the original position of the affected floor. The location of the fracture site of the affected floor was posterior to the posterior pole of the unaffected globe in this case (D).

The variables measured were displacements of orbital walls, displacement of the globe and relative location of the fracture site. Correlations between displacements of orbital walls and displacement of the globe were determined.

**Statistical analysis**

Statistical analyses were performed with Microsoft Office EXCEL 2010 (Microsoft, Redmond, WA, USA) and spss 17.0 (SPSS, Chicago, IL, USA). The measured values were recorded as mean ± SD. One-sample *t*-test was conducted to confirm whether the displacements of the globe were significant (*p*-value <0.05) in certain types of orbital blowout fracture. Correlation analysis was conducted between the displacements of orbital walls and the displacement of the globe. *p*-Value <0.05 was considered statistically significant. Regression formula was fitted for the variables that had significant correlation. Constant is not included in the formula according to its clinical application.

**Results**

One hundred forty-four adult Chinese (83 men, 61 women), aged 22–66 years (median = 38) at the time of trauma, were included in this study. The interval between the onset of trauma and CT examination was 30 days to 10 years (median = 65 days). Sixty-seven patients had blowout fractures of the right orbit and 77 of the left orbit. Forty-three patients had pure medial-wall fracture, 28 had pure floor fracture, and 73 had medial-wall and floor fractures. All patients received only conservative treatment for orbital fracture before the CT examination.

The location of the fracture site was compared with the position of the unaffected globe (Table 1). Ninety-nine per cent of fracture sites of the medial wall and 100% of fracture sites of the floor were posterior to the centre of the unaffected globe, more than half of which were posterior to the posterior pole of the globe.

Displacements of orbital walls and the globe in various types of orbital

blowout fractures are listed in Table 2. The globe moved significantly medially (*p* < 0.001) and backwards (*p* < 0.001) in pure medial-wall fracture; backwards (*p* < 0.001) and downwards (*p* = 0.017) in pure floor fracture; and medially (*p* < 0.001), backwards (*p* < 0.001) and downwards (*p* < 0.001) in medial-wall and floor fractures. Horizontal, antero-posterior and vertical displacements of the globe were correlated with the displacements of orbital walls. Regression formulae were fitted separately for male and female subjects (Table 3). Application of the formulae revealed that the same amount of displacement of orbital walls caused more severe medial, backward and downward displacement of the globe in female patients than in male patients.

**Discussion**

Displacement of the globe is a key factor of decision-making in management of orbital blowout fractures. According to the literature and clinical experience, enophthalmos greater than 2–3 mm becomes clinically noticeable (Hazani & Yaremchuk 2012; Zhang et al. 2012; Boyette et al. 2015) and requires surgical correction preferably within 2 weeks of the injury (Courtney et al. 2000; Zhang et al. 2012; Boyette et al. 2015; Choi et al. 2016b; Yamanaka et al. 2018). However, intraorbital oedema occurs early after fracture and masks the exact displacement of the globe (Whitehouse et al. 1994; Yab et al. 1997; Courtney et al. 2000; Lee & Lee 2016). Thus, measurements of the extent of fracture have been used to predict the extent of late enophthalmos after orbital fracture (Whitehouse et al. 1994; Yab et al. 1997; Ramieri et al. 2000; Cunningham et al. 2005; Zhang et al. 2012; Sung et al. 2013;

**Table 1.** Relative location of the fracture site to the position of the unaffected globe.

Type of orbital blowout fracture	Orbital wall of fracture	Relative location of the fracture site to the position of the unaffected globe		
		Anterior to the globe centre	Posterior to the globe centre and anterior to the posterior pole of the globe	Posterior to the posterior pole of the globe
Pure medial-wall fracture (43 subjects)	Medial wall	0 (0%)	15 (34.88%)	28 (65.12%)
Pure floor fracture (28 subjects)	Floor	0 (0%)	7 (25.00%)	21 (75.00%)
Medial-wall and floor fractures (73 subjects)	Medial wall	1 (1.37%)	26 (35.62%)	46 (63.01%)
	Floor	0 (0%)	32 (43.84%)	41 (56.16%)

**Table 2.** Displacements of orbital walls and globe in types of orbital blowout fractures.

Type of orbital blowout fracture	Displacement of orbital medial wall (mean ± SD)	Displacement of orbital floor (mean ± SD)	Displacements of the globe (mean ± SD) (one-sample <i>t</i> -test*)		
			Medial horizontal displacement (mm)	Backward anteroposterior displacement (mm)	Downward vertical displacement (mm)
Pure medial-wall fracture (43 subjects)	8.76 ± 3.39	12.79 ± 5.12	1.55 ± 0.95 ( <i>t</i> = 10.671, <i>p</i> < 0.001)	1.53 ± 1.18 ( <i>t</i> = 8.488, <i>p</i> < 0.001)	0.32 ± 1.30 ( <i>t</i> = 1.631, <i>p</i> = 0.110)
Pure floor fracture (28 subjects)			0.05 ± 0.79 ( <i>t</i> = 0.320, <i>p</i> = 0.751)	1.79 ± 0.95 ( <i>t</i> = 9.953, <i>p</i> < 0.001)	0.62 ± 1.29 ( <i>t</i> = 2.543, <i>p</i> = 0.017)
Medial-wall and floor fractures (73 subjects)	8.90 ± 3.7	8.79 ± 4.55	1.93 ± 1.16 ( <i>t</i> = 14.280, <i>p</i> < 0.001)	2.92 ± 1.48 ( <i>t</i> = 16.912, <i>p</i> < 0.001)	1.25 ± 1.50 ( <i>t</i> = 7.140, <i>p</i> < 0.001)

\* One-sample *t*-test was conducted for comparisons of the displacements of the globe and zero. *p* < 0.05 indicates that the displacements were statistically significant.



**Table 3.** Correlation between displacements of orbital walls and displacement of the globe.

Independent variable ( <i>a</i> , <i>b</i> )	Dependent variable ( <i>y</i> )	Sex (83 males, 61 females)	<i>p</i> *	<i>r</i>	Regression formula <sup>†</sup>
<i>a</i> = medial horizontal displacement of orbital medial wall (mm)	Medial horizontal displacement of the globe (mm)	Male	<0.001 ( <i>y</i> with <i>a</i> ) 0.236 ( <i>y</i> with <i>b</i> )	0.729 ( <i>y</i> with <i>a</i> )	0.131 ( <i>y</i> with <i>b</i> ) $y = 0.18a$
		Female	<0.001 ( <i>y</i> with <i>a</i> ) 0.194 ( <i>y</i> with <i>b</i> )	0.873 ( <i>y</i> with <i>a</i> )	0.168 ( <i>y</i> with <i>b</i> ) $y = 0.20a$
<i>b</i> = downward vertical displacement of orbital floor (mm)	Backward anteroposterior displacement of the globe (mm)	Male	<0.001 ( <i>y</i> with <i>a</i> ) <0.001 ( <i>y</i> with <i>b</i> )	0.703 ( <i>y</i> with <i>a</i> ) 0.902 ( <i>y</i> with <i>a</i> & <i>b</i> )	0.744 ( <i>y</i> with <i>b</i> ) $y = 0.16a + 0.15b$
		Female	<0.001 ( <i>y</i> with <i>a</i> ) <0.001 ( <i>y</i> with <i>b</i> )	0.818 ( <i>y</i> with <i>a</i> ) 0.933 ( <i>y</i> with <i>a</i> & <i>b</i> )	0.725 ( <i>y</i> with <i>b</i> ) $y = 0.18a + 0.15b$
	Downward vertical displacement of the globe (mm)	Male	0.009 ( <i>y</i> with <i>a</i> ) 0.036 ( <i>y</i> with <i>b</i> )	0.286 ( <i>y</i> with <i>a</i> ) 0.470 ( <i>y</i> with <i>a</i> & <i>b</i> )	0.230 ( <i>y</i> with <i>b</i> ) $y = 0.06a + 0.04b$
		Female	<0.001 ( <i>y</i> with <i>a</i> ) <0.001 ( <i>y</i> with <i>b</i> )	0.427 ( <i>y</i> with <i>a</i> ) 0.726 ( <i>y</i> with <i>a</i> & <i>b</i> )	0.472 ( <i>y</i> with <i>b</i> ) $y = 0.07a + 0.09b$

\* In correlation analysis, *p* < 0.05 indicates that the correlation between these variables was significant.

<sup>†</sup> Regression formula is fitted for the variables that had significant correlation (*p* < 0.05). The constant is not included in the formula according to the clinical application of the formula.

Choi et al. 2016a,b; Lee & Lee 2016; Cha et al. 2017; Sugiura et al. 2017). One millilitre of increased orbital volume can cause enophthalmos of 0.8 mm (Whitehouse et al. 1994), and a fracture defect of 2.75 cm<sup>2</sup> can cause enophthalmos of 2 mm (Sung et al. 2013). However, clinical application of these predictive models is limited because image processing of area or volume is demanding and not feasible with ordinary CT browsers. Therefore, in this study, we built a linear measuring method and used it instead of area or volume measurements. Although linear measurements might be less concrete than area and volume measurements, they are more practical in clinical use.

According to the hydraulic mechanism of orbital blowout fractures, the force to the globe reaches the orbital walls, breaking the thin medial wall/floor and resulting in displacement of the wall segment and soft tissue into the ethmoid/maxillary sinuses (Waterhouse et al. 1999; He et al. 2012). Fractures of the orbital roof and lateral wall are less frequent than medial-wall and floor fractures and generally do not cause herniation of intraorbital content into the sinus, so they were not included in this study. Linear measurement of the farthest displacement of the fractured orbital wall is a variable to reflect the extent of fracture (Cunningham et al. 2005; Lee & Lee 2016; Cai et al. 2018). We measured horizontal displacement of the medial wall and vertical displacement of floor, with the unaffected orbit as the control. Since the measurements were along co-ordinate axes, they were the same in coronal, horizontal and sagittal

views. This measuring method is feasible with ordinary CT browsers used in clinical practice.

We found that various types of orbital blowout fracture had variable features in displacement of the globe. The globe moved medially and backwards in pure medial-wall fractures; backwards and downwards in pure floor fractures; and medially, backwards and downwards in medial-wall and floor fractures. Displacement of the globe was correlated with displacement of the orbital walls, and the regression formulae were fitted accordingly. From the formulae, we learned that only displacement of the medial wall could cause medial displacement of the globe; displacement of both the medial wall and floor could cause backward and downward displacement of the globe, but the extent of downward displacement was much less severe than that of backward displacement. These formulae were similar to those used in a previous study (Lee & Lee 2016). In that study, about 2.0 mm of enophthalmos was associated with 9.3- and 10.0-mm enophthalmos estimate lines in patients with isolated inferior-wall fractures and medial-wall fractures, respectively. To note, the enophthalmos estimate lines in that study were perpendicular to the defect line but not along the horizontal or vertical axis, so they were not equal to the displacement of orbital walls in this study. Further, the enophthalmos estimate lines were measured differently in coronal, horizontal and sagittal views, whereas the displacement of orbital walls in this study had the same measurement in these views. The formulae

generated in this study can therefore be used in clinical practice to predict the direction and extent of late displacement of the globe by measuring the displacement of orbital walls in early cases.

In comparing the location of the fracture site with the position of the unaffected globe, we found that most fracture sites were posterior to the globe centre, more than half of which were posterior to the posterior pole of the globe. This finding was consistent with the hydraulic mechanism and the biomechanical analysis of orbital blowout fracture as reported (Waterhouse et al. 1999; Schaller et al. 2013) and indicated the most fragile sites in orbital walls. Further, the relative posterior positions of the fracture sites in both medial-wall fractures and floor fractures explain why the fractures of orbital walls can lead to significant backward displacement of the globe.

Previous studies found that the orbit is smaller in females than in males (Ji et al. 2010, 2018; Regensburg et al. 2011). In this study, displacement of the globe after orbital blowout fracture also differed between sexes. Application of the formulae revealed that with the same amount of displacement of orbital walls, the globe was displaced more in females than in males. This finding was consistent with the gender differences found in previous studies because the enlargement of orbital cavity caused by fracture would interfere more with the position of intraorbital contents in small orbits than in big ones.

We acknowledge that our study has some limitations. (1) Only unilateral fracture cases were included because

the unaffected side served as a control to determine the original position of the affected side. In clinical cases, if the original position of the fracture site could be determined by connecting the edges of the bony defect, the formulae would also be applicable to bilateral fracture cases. (2) The study included late cases of orbital fracture (CT examination at least 30 days after trauma) because the displacement of orbital walls and the late displacement of the globe could therefore be measured in the same CT scans. It does not mean that the results are only suitable for late cases. On the contrary, the formulae worked out in this study are aimed to predict the late displacement of the globe by measuring the displacement of orbital walls in early cases. (3) The study subjects had no orbital disease other than the orbital fracture and were already adults at the time of trauma, so their bony orbits were presumed to have no significant change or growth during the time interval between the fracture and the CT examination; as all the subjects were adults, the results of the study are only applicable to adult cases. (4) Children's orbits are smaller than adults' orbits (Bentley et al. 2002; Ji et al. 2015), so it can be presumed that the same amount of displacement of the orbital walls causes more displacement of the globe in children than in adults; this assumption should be verified with study of orbital fractures in paediatric patients.

## Conclusions

We established a linear measuring method to predict late displacement of the globe in orbital blowout fractures. Displacement of the globe was correlated with displacements of the orbital walls. The fracture sites were mostly posterior to the centre of the unaffected globe. The same extent of fracture caused more displacement of the globe in female patients than in male patients. The regression formulae could be predictive models, suitable for clinical application.

## References

Bentley RP, Sgouros S, Natarajan K, Dover MS & Hockley AD (2002): Normal changes in orbital volume during childhood. *J Neurosurg* **96**: 742–746.

Boyette JR, Pemberton JD & Bonilla-Velez J (2015): Management of orbital fractures: challenges and solutions. *Clin Ophthalmol* **9**: 2127–2137.

Brady SM, McMann MA, Mazzoli RA, Bushley DM, Ainbinder DJ & Carroll RB (2001): The diagnosis and management of orbital blowout fractures: update 2001. *Am J Emerg Med* **19**: 147–154.

Cai EZ, Chong XT, Ong WL, Chan LSF, Goh JY, Sundar G & Lim TC (2018): Planes of reference for orbital fractures: a technique for reproducible measurements of the orbit on computed tomography scans. *J Craniofac Surg* **29**: 1817–1820.

Catone GA, Morrissette MP & Carlson ER (1988): A retrospective study of untreated orbital blowout fractures. *J Oral Maxillofac Surg* **46**: 1033–1038.

Cha JH, Moon MH, Lee YH, Koh IC, Kim KN, Kim CG & Kim H (2017): Correlation between the 2-dimensional extent of orbital defects and the 3-dimensional volume of herniated orbital content in patients with isolated orbital wall fractures. *Arch Plast Surg* **44**: 26–33.

Choi J, Park SW, Kim J, Park J & Kim JS (2016a): Predicting late enophthalmos: differences between medial and inferior orbital wall fractures. *J Plast Reconstr Aesthet Surg* **69**: e238–e244.

Choi SH, Kang DH & Gu JH (2016b): The Correlation between the orbital volume ratio and enophthalmos in unoperated blowout fractures. *Arch Plast Surg* **43**: 518–522.

Courtney DJ, Thomas S & Whitfield PH (2000): Isolated orbital blowout fractures: survey and review. *Br J Oral Maxillofac Surg* **38**: 496–504.

Cunningham LL, Peterson GP & Haug RH (2005): The relationship between enophthalmos, linear displacement, and volume change in experimentally recreated orbital fractures. *J Oral Maxillofac Surg* **63**: 1169–1173.

Hazani R & Yaremchuk MJ (2012): Correction of posttraumatic enophthalmos. *Arch Plast Surg* **39**: 11–17.

He Y, Zhang Y & An JG (2012): Correlation of types of orbital fracture and occurrence of enophthalmos. *J Craniofac Surg* **23**: 1050–1053.

Ji Y, Qian Z, Dong Y, Zhou H & Fan X (2010): Quantitative morphometry of the orbit in Chinese adults based on a three-dimensional reconstruction method. *J Anat* **217**: 501–506.

Ji Y, Ye F, Zhou H, Xie Q, Ge S & Fan X (2015): Bony orbital maldevelopment after enucleation. *J Anat* **227**: 647–653.

Ji Y, Lai C, Gu L & Fan X (2018): Measurement of intra-orbital structures in normal chinese adults based on a three-dimensional coordinate system. *Curr Eye Res* **43**: 1477–1483.

Lee HB & Lee SH (2016): A straightforward method of predicting enophthalmos in blowout fractures using enophthalmos estimate line. *J Oral Maxillofac Surg* **74**: 2457–2464.

Lundström A & Lundström F (1995): The Frankfort horizontal as a basis for cephalometric analysis. *Am J Orthod Dentofacial Orthop* **107**: 537–540.

Ramieri G, Spada MC, Bianchi SD & Berrone S (2000): Dimensions and volumes of the orbit and orbital fat in posttraumatic enophthalmos. *Dentomaxillofac Radiol* **29**: 302–311.

Regensburg NI, Wiersinga WM, van Velthoven ME, Berendschot TT, Zonneveld FW, Baldeschi L, Saeed P & Mourits MP (2011): Age and gender-specific reference values of orbital fat and muscle volumes in Caucasians. *Br J Ophthalmol* **95**: 1660–1663.

Schaller A, Huempfer-Hierl H, Hemprich A & Hierl T (2013): Biomechanical mechanisms of orbital wall fractures - a transient finite element analysis. *J Craniomaxillofac Surg* **41**: 710–717.

Sugiura K, Yamada H, Okumoto T, Inoue Y & Onishi S (2017): Quantitative assessment of orbital fractures in Asian patients: CT measurement of orbital volume. *J Craniomaxillofac Surg* **45**: 1944–1947.

Sung YS, Chung CM & Hong IP (2013): The Correlation between the degree of enophthalmos and the extent of fracture in medial orbital wall fracture left untreated for over six months: a retrospective analysis of 81 cases at a single institution. *Arch Plast Surg* **40**: 335–340.

Waterhouse N, Lyne J, Urdang M & Garey L (1999): An investigation into the mechanism of orbital blowout fractures. *Br J Plast Surg* **52**: 607–612.

Whitehouse RW, Batterbury M, Jackson A & Noble JL (1994): Prediction of enophthalmos by computed tomography after "blowout" orbital fracture. *Br J Ophthalmol* **78**: 618–620.

Yab K, Tajima S & Ohba S (1997): Displacements of eyeball in orbital blowout fractures. *Plast Reconstr Surg* **100**: 1409–1417.

Yamanaka Y, Watanabe A, Sotozono C & Kinoshita S (2018): Impact of surgical timing of postoperative ocular motility in orbital blowout fractures. *Br J Ophthalmol* **102**: 398–403.

Zhang Z, Zhang Y, He Y, An J & Zwahlen RA (2012): Correlation between volume of herniated orbital contents and the amount of enophthalmos in orbital floor and wall fractures. *J Oral Maxillofac Surg* **70**: 68–73.

Received on March 2nd, 2019.

Accepted on July 23rd, 2019.

### Correspondence:

Xianqun Fan  
 Department of Ophthalmology  
 Shanghai Ninth People's Hospital  
 Shanghai Jiao Tong University School of  
 Medicine  
 639 Zhizaoju Road  
 Shanghai 200011  
 China  
 Tel: +86-21-23271699-5587  
 Fax: +86-21-63137148  
 Email: fanxq@sjtu.edu.cn  
 and  
 Lixu Gu  
 School of Biomedical Engineering  
 Shanghai Jiao Tong University  
 800 Dongchuan Road  
 Shanghai 200241  
 China  
 Tel: +86-21-62933250  
 Fax: +86-21-62933250  
 Email: gulixu@sjtu.edu.cn

### Source of funding

The National Natural Science Foundation of China (31600971), the National Key Research and Development Program of China (2018YFC1106101, 2018YFC1106100, 2016YFC0106200), the 863 national research fund of China (2015AA043203), and the Science and Technology Commission of Shanghai (17DZ2260100). The funding organization had no role in the design or conduct of this research.